ELSEVIER

Materials Science and Engineering A 393 (2005) 36–41

MATERIALS SCIENCE & ENGINEERING A

www.elsevier.com/locate/msea

The effect of composition on microstructure and properties of PNW–PMS–PZT ceramics for high-power piezoelectric transformer

Hong-liang Du[a], Shao-bo Qu[b,c,*], Jun Che[b,c], Zhi-yi Liu[c], Xiao-yong Wei[b], Zhi-bin Pei[c]

[a] *The College of Engineering, Air Force Engineering University, Xi'an 710038, China*
[b] *Electronic Materials Research Laboratory, Key Laboratory of Educational Ministry, Xi'an Jiaotong University, Xi'an 710049, China*
[c] *The Department of Applied Maths and Physics, the College of Science, Air Force Engineering University, Xi'an 710051, China*

Received 21 June 2004; received in revised form 23 September 2004; accepted 24 September 2004

Abstract

$(Pb_{0.95}Sr_{0.05})[(Mn_{1/3}Sb_{2/3})_x(Ni_{1/2}W_{1/2})_y(Zr_{1/2}Ti_{1/2})_z]O_3$ piezoelectric ceramics (abbreviated as PNW–PMS–PZT) with 1 mol% excess PbO, 0.25 wt% CeO_2 and 0.2 wt% MnO_2were synthesized by traditional ceramics process. The effect of $Pb(Mn_{1/3}Sb_{2/3})O_3$ (abbreviated as PMS) and $Pb(Ni_{1/2}W_{1/2})O_3$ (abbreviated as PNW) on phase structure, dielectric and piezoelectric properties was investigated in detail. The content of perovskite phase of all ceramics specimens is 100%, the phase structure of PNW–PMS–PZT ceramics changed from tetragonal phase to single rhombohedral phase with the amount of PMS and PNW increased. Take into consideration dielectric constant, ε_r, dielectric loss tan δ, electromechanical coupling factor k_p, mechanical quality factor Q_m, Curie temperature T_c and sintering temperature, it was concluded that the ceramics with composition of $x = 0.06$, $y = 0.02$, $z = 0.92$ can be used for high-power piezoelectric transformer. These properties include $\varepsilon_r = 2138$, $\tan\delta = 0.0058$, $k_p = 0.613$, $Q_m = 1275$, $d_{33} = 380$ pC/N, $T_c = 205\,^{\circ}$C.

Keywords: PNW–PMS–PZT piezoelectric ceramics; Dielectric properties; Piezoelectric properties; High-power; Piezoelectric transformer

1. Introduction

Piezoelectric transformer has been studied for many years [1]. Recently, it is actively researched mainly to increase to step-up ratio and the output power [2–5]. Piezoelectric transformer has several advantages over the conventional magnetic transformer [6,7]. First, the piezoelectric transformer can be miniaturized to a greater degree since the energy stored by the elastic vibration is larger than in the magnetic transformers. In addition, because there are no wire windings, the transformers are nonflammable and safe with regard to potential short-circuiting of the output terminal. Moreover, magnetic shield is not necessary in piezoelectric transformers. However, since conventional Rosen-type piezoelectric transformer for liquid crystal display backlight operated at high voltage and low current, these output power is only 2–3 W [2,8], they can not be successfully used for illuminating general fluorescent lamps because low voltage and high current are required. Therefore, a new type of high power transformer is necessary for the ballasts of the lamps. It is necessary for enhancing piezoelectric transformer output power to have higher output current, its output capacitance must be high in order to achieve high output current. Therefore, the piezoelectric ceramics for high-power piezoelectric transformer must have higher dielectric constant ε_r [8]. In addition, to achieve high power the piezoelectric transformer, it is necessary to have a high mechanical quality factor Q_m because the piezoelectric transformer operated at its resonant frequency under a high input voltage leads to the temperature rise and the deterioration of piezoelectric properties with the increase of its vibration velocity [8–10]. Consequently, the ceramics used for high-power transformer must have higher Q_m and lower tan. Moreover, higher k_p is necessary to increase step-up ratio [11].

Gao et al. [12] had shown $Pb(Mn_{1/3}Sb_{2/3})O_3$–Pb(Ti, Zr)O_3 (abbreviated as PMS–PZT) piezoelectric ceramics

* Corresponding author.
E-mail address: qushaobo@126.com (S.-b. Qu).

0921-5093/$ – see front matter © 2004 Published by Elsevier B.V.
doi:10.1016/j.msea.2004.09.046

have higher k_p, Q_m and higher maximum velocities than Pb(Ti,Zr)O_3 (abbreviated as PZT), however, ε_r of PMS–PZT piezoelectric ceramics is only 660. Yoo et al. had shown Pb($Ni_{1/2}W_{1/2}$)O_3 (abbreviated as PNW) added to Pb($Mn_{1/3}Nb_{2/3}$)O_3–Pb(Ti, Zr)O_3 ceramics can increase the dielectric constant and decrease the sintering temperature of Pb($Ni_{1/2}W_{1/2}$)O_3–Pb($Mn_{1/3}Sb_{2/3}$)O_3–Pb(Ti, Zr)O_3 ceramics [8], so this work added PNW to PMS–PZT to increase the dielectric constant and decrease the sintering temperature.

Yoo et al. [8] had reported that 0.25 wt% CeO_2 additive can improve the temperature coefficient of resonant frequency Tcf_r, and that 0.2 mol% Sr substitution for Pb can increase Q_m, Chen et al. [13] had reported that suitable Mn doping can significantly improve Q_m and slightly decrease k_p, so 0.25 wt% CeO_2, 5 mol% $SrCO_3$ and 0.2 wt% MnO_2 was added in this study. In addition, 1 mol% excess PbO was added to eliminate pyrochlore phase and compensate for PbO loss during sintering process [14].

The purpose of this paper is to investigate the effect of composition on microstructure and properties of PNW–PMS–PZT composition ceramics, and to provide promising candidates for high-power piezoelectric transformer.

2. Experimental procedure

The specimens studied in this research were fabricated according to formula: $(Pb_{0.95}Sr_{0.05})[(Mn_{1/3}Sb_{2/3})_x(Ni_{1/2}W_{1/2})_y(Zr_{1/2}Ti_{1/2})_z]O_3 + 0.25$ wt%$(CeO_2) + 1$ mol% excess $(PbO) + 0.2$ wt% (MnO_2), $x + y + z = 1$, where $x = 0.05$–0.08; $y = 0.01$–0.04; $z = 0.90$–0.93, respectively. The chemical compositions of each specimen are listed in Table 1. The specimens were prepared by traditional ceramics process and reagent-grade Pb_3O_4, ZrO_2, TiO_2, $SrCO_3$, NiO, WO_3, MnO_2, Sb_2O_3 and CeO_2 powders were acetone-milled for 12 h in a zirconia ball mill and then calcined at 850 °C for 2 h. The calcined powders were ground, ball-milled again and pressed into disks using PVA as a binder. After burning off PVA, the pellets were sintered in a sealed alumina crucible at different soaking temperature (from 1075 to 1200 °C) for 2 h. In order to compensate for PbO loss from the pellets, a PbO-rich atmosphere was maintained by placing an equi-molar mixture of PbO and ZrO_2 inside the covered alumina crucible.

Table 1
Chemical composition of specimens investigated in this study

Samples	Composition		
	x	*y*	*z*
#1	0.05	0.02	0.93
#2	0.06	0.02	0.92
#3	0.07	0.02	0.91
#4	0.08	0.02	0.90
#5	0.06	0.01	0.93
#6	0.06	0.03	0.91
#7	0.06	0.04	0.90

The apparent density of the sintered specimens was calculated from the volume and weight. The phase structure of the sintered ceramics was analyzed by using a Rigaku D/Max-2400 diffractomerer using Cu Kα radiation. The fractured surfaces were examined by scanning electron microscopy (HITACHI S-2700).

The specimens were polished for the dielectric and piezoelectric studies. Silver paste was fired on both sides of the samples at 560 °C for 10 min as the electrodes for the dielectric and piezoelectric measurements. The dielectric response was measured at the frequency of 1 kHz using an automatic LCR meter (WK4225) at a temperature range from 40 to 350 °C. The samples were poled in 120 °C silicon oil bath by applying a DC electric field of 3 kV/mm for 30 min. Piezoelectric properties were measured by the resonance-antiresonance method on the basis of IEEE standards using an impedance analyzer (HP4294A).

3. Results and discussion

3.1. Phases analysis

Fig. 1 shows X-ray diffraction (XRD) patterns of specimens sintered at 1150 °C. The content of perovskite phase of all ceramics specimens is 100%. It is noted that the peak splitting at (2 0 0) plane position weakens gradually as the concentration of PMS and PNW increased, to highlight this progress, XRD peaks of $2\theta = 45°$ versus the amount of PMS and PNW are shown in Figs. 2 and 3, respectively. There are two possible reasons for weakening of splitting at (2 0 0) plane position. First, incorporation of Mn^{2+} into B-site of perovskite-structured morphotropic phase boundary (MPB) composition stabilizes rhombohedral phase against tetragonal one [15]. Moreover, the addition of PMS and PNW shifts the MPB region towards $PbZrO_3$-rich side at room temperature.

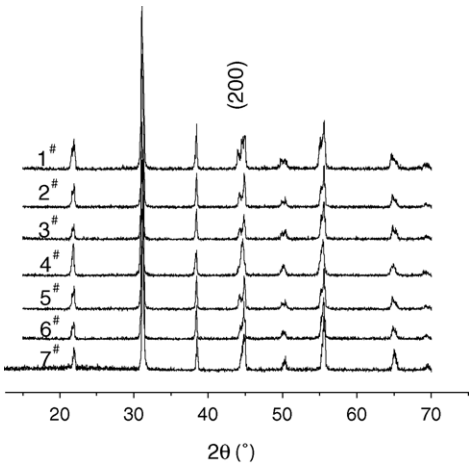

Fig. 1. XRD patterns of the specimens sintered at 1150 °C.

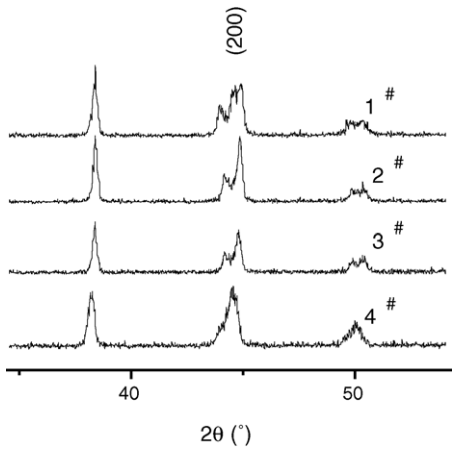

Fig. 2. XRD peaks of $2\theta = 45^\circ$ vs. the concentration of PMS in PNW–PMS–PZT ceramics with 2 mol% PNW.

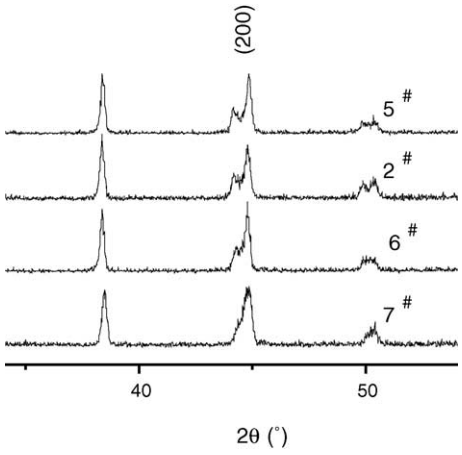

Fig. 3. XRD peaks of $2\theta = 45^\circ$ vs. the concentration of PNW in PNW–PMS–PZT ceramics with 6 mol% PMS.

3.2. Physical properties and microstructure

Fig. 4 shows the sintering temperature and the amount of PMS and PNW dependence of the apparent density. Fig. 5 shows the SEM photos of the fractured surface of specimens with 1–4 mol% PNW. The grain size of #5 sample with 1 mol% PNW is only 2 μm and there are pores in it. However, the grain size significantly increased with increasing the content of PNW from 2 to 4 mol%. In addition, small quantities of substance associated with PNW exsolution was observed near the grain boundaries in #7 specimen with 4 mol% PNW. This result indicates that PNW have a limited solubility in PMS–PZT ceramics, tending to exsolve at concentration about 3 mol%.

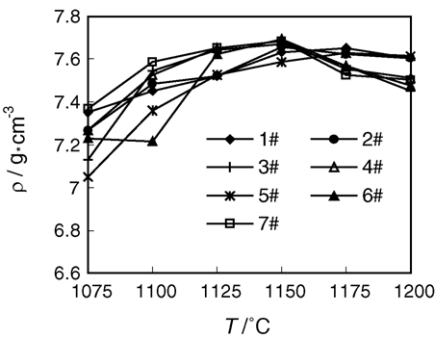

Fig. 4. The apparent density of PNW–PMS–PZT ceramic as a function of sintering temperature.

3.3. Dielectric properties

Figs. 6 and 7 show the content of PMS and PNW dependence of dielectric constant and dielectric loss at room temperature respectively. Dielectric constant of PNW–PMS–PZT piezoelectric ceramics is three times larger than one of PMS–PZT piezoelectric ceramics. There are three possible reasons for the increase of ε_r. First and foremost, PNW with high ε_r was added into PMS–PZT ceramics. Second, the grain growth made the dielectric constant increase because it led to a reduction in the number of grain boundary [16]. Third, Curie temperature of PNW–PMS–PZT ceramics moved towards lower temperature side owing to PNW with lower Curie temperature added. With the content of PMS increased, ε_r decreased and $\tan\delta$ increased gradually, because more oxygen vacancies would be generated to balance the charge, when more Mn^{2+} are incorporated into B-site of perovskite structure. It is well known that these oxygen vacancies can inhibit the domain or microdomain wall move, consequently, ε_r decreased and $\tan\delta$ increased gradually with the content of PMS increased. When the content of PNW was <2 mol%, ε_r and $\tan\delta$ increased with the content of PNW increased. When the content of PNW was >3 mol%, ε_r and $\tan\delta$ decreased gradually with the content of PNW increased. Because the domain or microdomain wall reorient easily owing to the grain growth with the content of PNW increased, when PNW was added more than 3 mol%, the excess PNW will stay in the boundary and form a grain boundary layer, ε_r decreased because of grain boundary layer.

Figs. 8 and 9, respectively show dielectric constant as a function of the content of PMS, PNW and temperature. As the content of PMS and PNW increased in the system, T_c gradually decreased, this is due to the decrease of amount of PZT that has the relative high Curie temperature of 386 °C [17]. Peak dielectric constant increased with the content of PMS increased. Because the increase of the content of PMS results in the increase of oxygen vacancies, with temperature increased, the thermal energy may be sufficient to eliminate inhibition to the domain or microdomain wall by oxygen vacancies. Peak dielectric constant decreased with the content of PNW increased. This is due to the effect of the volume proportion of grain boundary was eliminated with temperature increased, in addition, peak dielectric constant decreased because of grain boundary layer.

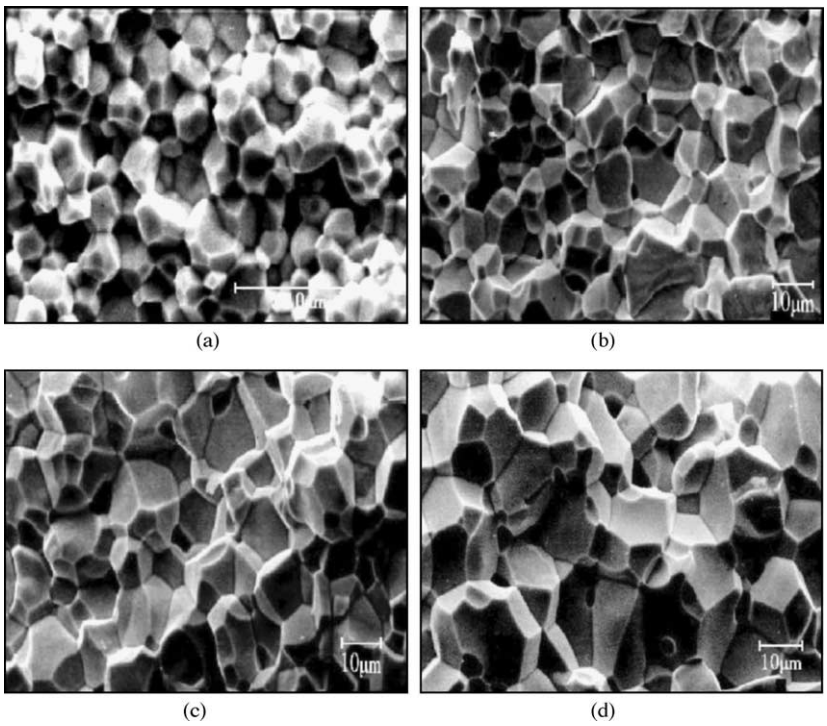

Fig. 5. SEM photographs of the fractured surface of the sintered specimens with 6 mol% PMS as the different the content of PNW: (a) 1 mol% PNW, (b) 2 mol% PNW, (c) 3 mol% PNW, (d) 4 mol% PNW.

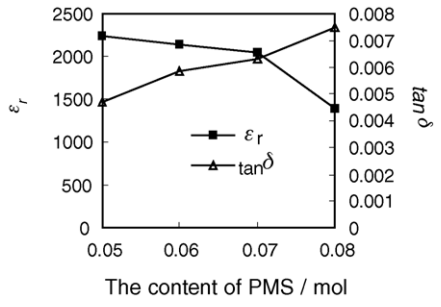

Fig. 6. ε_r and tan δ (1 kHz) of PNW–PMS–PZT ceramics with 2 mol% PNW as the different concentration of PMS.

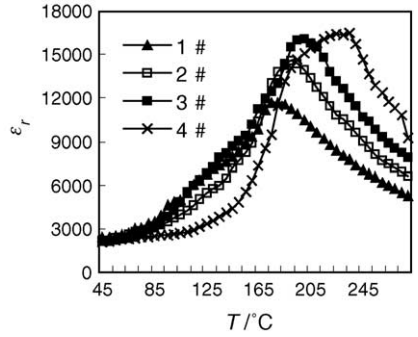

Fig. 8. Temperature dependence of ε_r (1 kHz) for specimens #1–4.

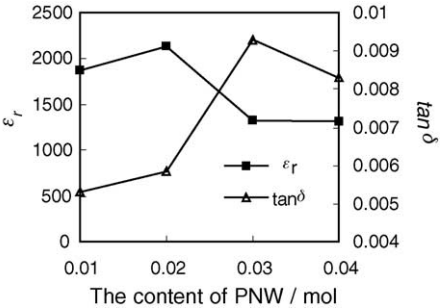

Fig. 7. ε_r and tan δ (1 kHz) of PNW–PMS–PZT ceramics with 6 mol% PMS as the different concentration of PNW.

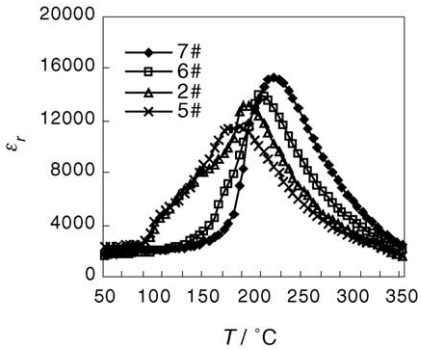

Fig. 9. Temperature dependence of ε_r (1 kHz) for specimens #5, #2, #6 and #7.

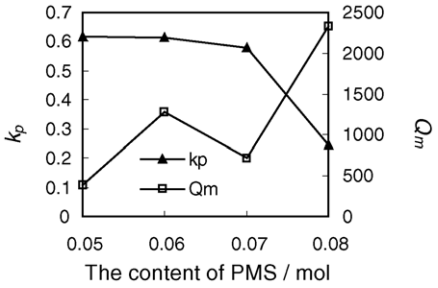

Fig. 10. k_p and Q_m of PNW–PMS–PZT ceramics with 2 mol% PNW as different the content of PMS.

3.4. Piezoelectric properties

Figs. 10 and 11 show respectively k_p, Q_m and d_{33} as a function of the content of PMS. With the content of PMS increased, k_p, d_{33} decreased and Q_m increased. There are two possible reasons. First, previous investigations have demonstrated that PMS–PZT ceramics has "hard" piezoelectric characteristics [10], more and more oxygen vacancies are introduced into PNW–PMS–PZT ceramics owing to the increase of the content of PMS, the introduction of oxygen vacancies inhibited the domain wall mobility, which subsequently decreased k_p and d_{33}, increased Q_m. Second, the phase structure of PNW–PMS–PZT ceramics changed from the tetragonal phase to the coexistence of the rhombohedral and tetragonal phase, then to single rhombohedral, with the amount of PMS increased. Figs. 12 and 13 show respectively k_p, Q_m and d_{33} as a function of the content of PNW. When the content of PNW was <2 mol%, k_p and d_{33} increased with the amount of PNW increased. When the content of PNW was >3 mol%, k_p and d_{33} decreased with the amount of PNW increased. As mentioned above, when the content of PNW was <2 mol%, the grain growth made k_p and d_{33} increase because the domain or microdomain wall reorient easily owing to the grain growth, which led to a reduction in the number of grain boundary, however, when the amount of PNW is >3 mol%, the excess PNW will stay in the boundary and form a grain boundary layer, which inhibit the movement of domain wall, therefore, k_p and d_{33} decreased. Q_m decreased with the amount of PNW increased owing to the grain growth.

Table 2 summarizes the dielectric and piezoelectric properties of PNW–PMS–PZT ceramics with the different concentration of PMS and PNW. Table 3 summarizes the dielectric and piezoelectric properties of PZT, PMS–PZT and PNW–PMS–PZT piezoelectric ceramics.

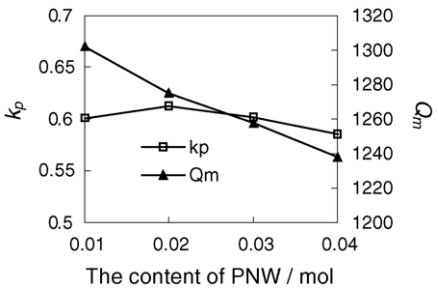

Fig. 11. k_p and Q_m of PNW–PMS–PZT ceramics with 6 mol% PMS as different the content of PNW.

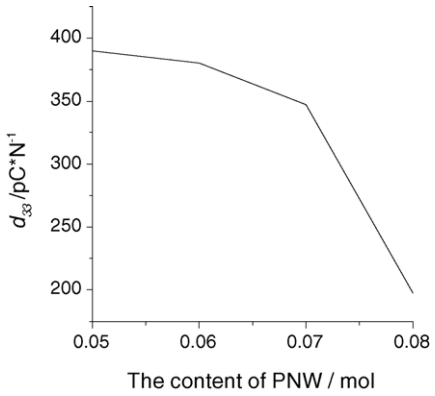

Fig. 12. d_{33} of PNW–PMS–PZT ceramics with 2 mol% PNW as different the content of PMS.

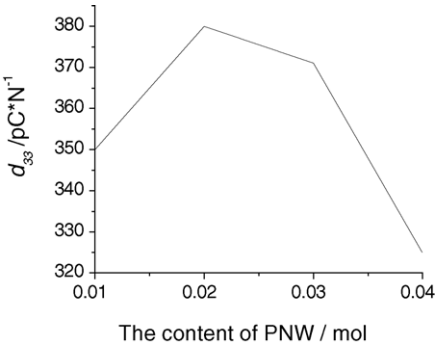

Fig. 13. d_{33} of PNW–PMS–PZT ceramics with 6 mol% PMS as different the content of PNW.

Take into consideration ε_r, $\tan\delta$, k_p and Q_m, it can be concluded that the composition of $x = 0.06$, $y = 0.02$, $z = 0.92$

Table 2
Dielectric and piezoelectric properties of PNW–PMS–PZT ceramics with the different concentration of PMS and PNW

Samples	ε_r	$\tan\delta$ (%)	T_c (°C)	k_p (%)	Q_m	d_{33} (pC/N)
#1	2234	0.47	225	61.7	393	390
#2	2138	0.584	205	61.3	1275	380
#3	2048	0.628	190	58.	718	347
#4	1392	0.748	175	24.5	2332	198
#5	1870	0.532	220	60.1	1303	350
#6	1328	0.929	190	60.2	1258	371
#7	1314	0.830	170	58.6	1238	325

Table 3
Dielectric and piezoelectric properties of PZT, PMS–PZT and PNW–PMS–PZT piezoelectric ceramics

Samples	ε_r	$\tan\delta$ (%)	T_c (°C)	k_p (%)	Q_m	d_{33} (pC/N)
PZT	460	0.500	350	37.5	1300	71
PMS–PZT	660	0.45	290	58	1150	230
PNW–PMS–PZT	2138	0.584	205	61.3	1275	380

(specimen #2) can be used for high-power piezoelectric transformer.

4. Conclusion

Dielectric and piezoelectric properties of PNW–PMS–PZT ceramics with 1 mol% excess PbO, 0.25 wt% CeO_2 and 0.2 wt% MnO_2 were investigated with the different concentration of PMS and PNW. The results are summarized as follows:

1 PNW–PMS–PZT piezoelectric ceramics with 100% perovskite phase were synthesized by traditional ceramics process for high-power piezoelectric transformer.
2 With the amount of PMS and PNW increased, the phase structure of PNW–PMS–PZT ceramics changed from tetragonal phase to the coexistence of the rhombohedral and tetragonal phase, then to single rhombohedral phase.
3 As the amount of PMS increased, ε_r, k_p and d_{33} decreased, $\tan\delta$ and Q_m gradually increased; when the content of PNW was <2 mol%, ε_r, $\tan\delta$, k_p and d_{33} increased with the amount of PNW increased. When the content of PNW was >3 mol%, ε_r, $\tan\delta$, k_p and d_{33} decreased with the amount of PNW increased, Q_m decreased all the while with the amount of PNW increased.
4 Take into consideration ε_r, $\tan\delta$, k_p, Q_m, T_c and sintering temperature, it can be concluded that the specimen #2 is the best one for high-power piezoelectric transformer applications ($\varepsilon_r = 2138$, $\tan\delta = 0.0058$, $k_p = 0.613$, $Q_m = 1275$, $d_{33} = 380$ pC/N, $T_c = 205\,^{\circ}$C).

Acknowledgements

This works was supported by Air Force Engineering University Foundation (serial number: 2002X08) and the Ministry of Sciences and Technology of China through 973-project under grant (serial number 2002CB613304).

References

[1] C.A. Rosen, Proc. Electron. Components Symp. (1957) 205.
[2] K. Kanayama, N. Maruko, Jpn. J. Appl. Phys. 36 (1997) 3048.
[3] K. Ishii, N. Akimoto, S. Tashirio, et al., Jpn. J. Appl. Phys. 37 (1998) 5330.
[4] J. Hu, Y. Fuda, M. Katsuno, et al., Jpn. J. Appl. Phys. 38 (1999) 3208.
[5] K. Sakarai, K. Ohnishi, K. Tomikawa, Jpn. J. Appl. Phys. 38 (1999) 5592–5597.
[6] J. Yoo, K. Yoon, Y. Lee, et al., Jpn. J. Appl. Phys. 39 (2000) 2680–2684.
[7] T. Futakuchi, H. Sugimori, K. Horii, et al., Jpn. J. Appl. Phys. 38 (1999) 3596–3599.
[8] J. Yoo, Y. Lee, K. Yoon, et al., Jpn. J. Appl. Phys. 40 (2001) 3256.
[9] S. Takahashi, S. Hirose, K. Uchino, J. Am. Ceram. Soc. 77 (1994) 2429.
[10] S. Tashiro, M. Ikehiro, H. Igarashi, Jpn. J. Appl. Phys. 36 (1997) 3004.
[11] L. Li, Y. Yao, Z. Mu, Ferroelectrics 28 (1980) 403–406.
[12] Y. Gao, Y.-H. Chen, J. Ryu, Jpn. J. Appl. Phys. 40 (2001) 687–693.
[13] Y.-H. Chen, S. Hirose, D. Viehland, et al., Jpn. J. Appl. Phys. 39 (2000) 4843–4852.
[14] F. Xia, X. Yao, J. Mater. Sci. 36 (2001) 247–253.
[15] W.Z. Zhu, M. Yan, J. Mater. Sci. Lett. 20 (2001) 1527–1529.
[16] R. Zuo, L. Li, R. Chen, et al., J. Mater. Sci. 35 (2000) 5433–5436.
[17] R.E. Eitel, C.A. Randall, T.R. Shrout, Jpn. J. Appl. Phys. 41 (2002) 2099.